Heat Transfer Coefficient in Viscous Three-Phase Inverse Fluidized Beds

S. M. Son, K. I. Lee, S. H. Kang, and Y. Kang
School of Chemical Engineering, Chungnam National University, Daejeon 305-764, Korea

S. D. Kim
Dept. of Chemical and Biomolecular Engineering, Korea Advanced Institute of Science Technology, Daejeon 305-701, Korea

DOI 10.1002/aic.11310
Published online September 26, 2007 in Wiley InterScience (www.interscience.wiley.com).

Keywords: heat transfer coefficient, viscous liquid medium, three-phase, inverse fluidized bed

Introduction

For the effective contacting among gas, liquid and solid phases in the beds with low density materials, inverse fluidization technology has been adopted in the chemical, biochemical, food and environmental processes such as ferrous iron oxidation, wastewater treatment, food fermentation processes, etc.[1–6] Because of rapidly growing applications, several investigations have been carried out on the three-phase inverse fluidized-bed reactors or contactors. The hydrodynamic characteristics such as bubble properties, flow regime, bed expansion, minimum liquid fluidization velocity, and transition velocity for the uniform fluidization have been examined.[7–11] Gas–liquid and liquid–solid mass transfer and liquid mixing in three-phase inverse fluidized beds have been also studied for the more practical applications in the industrial processes.[12–16]

Wastewater with floating materials and liquid phases in biochemical, pulp, and food processes have been generally viscous. In addition, low density suspension materials are frequently encountered in those processes. Moreover, sometimes the low density media particles with high porosity have been inserted into the continuous liquid medium for more efficient contacting, reaction, absorption, or adsorption in those heterogeneous processes. For the practical applications of three-phase inverse fluidized bed, of course, relevant information on the heat transfer in the bed with viscous liquid medium is essential, because the temperature in the reactor or process has to be controlled effectively in spite of complicated viscous heterogeneous contacting systems.[17,18] It has been understood that temperature control within a plausible level would be a fatal in the fields of food, biochemical, or wastewater treatment engineering employing the various kinds of microorganisms. However, there has been little attention on the heat transfer phenomena in three-phase inverse fluidized bed systems.[11]

In the present study, therefore, heat transfer phenomena were investigated in viscous three-phase inverse fluidized beds. Effects of gas and liquid velocities, liquid viscosity and particle density, and bed porosity on the immersed heater-to-bed heat transfer coefficient were determined. The heat transfer coefficients were correlated by means of dimensionless groups to be utilized for the design and scale-up of the system.

Experimental Studies

Experiments were carried out in an acrylic column 0.152 m in diameter and 2.5 m in height, as shown in Figure 1. A perforated plate, which contained 237 evenly spaced holes of diameter 3 mm, served as a liquid distributor with a stainless steel screen of 300 mesh.[11,15] The liquid distributor was installed at the top of the main column. The liquid phase was introduced to the liquid calming section through a 2.54-cm pipe from the liquid reservoir. The liquid distributor was situated between the main column section and a stainless steel box from which the liquid phase was withdrawn downward.

Correspondence concerning this article should be addressed to Y. Kang at kangyong@cnu.ac.kr.

© 2007 American Institute of Chemical Engineers

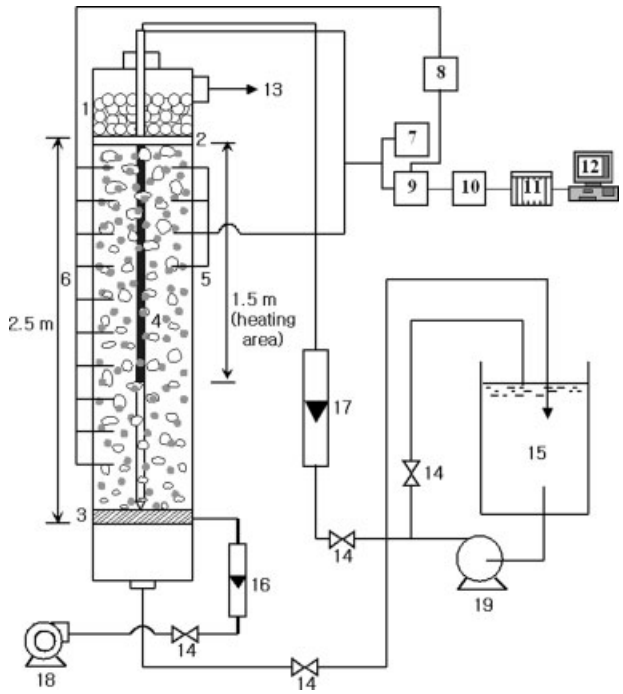

Figure 1. Experimental apparatus.

1. Liquid calming section, 2. Liquid distributor, 3. Gas distributor, 4. Heater, 5. Thermocouples, 6. Pressure taps, 7. Temperature indicator, 8. P-sensor, 9. Amplifier, 10. Low-pass filter, 11. A/D convertor, 12. Computer, 13. Vent line, 14. Control valve, 15. Reservior, 16. Gas flowmeter, 17. Liquid flowmeter, 18. Air compressor, 19. Liquid pump.

At the bottom, the gas was fed to the column through four evenly spaced 0.63-cm distributor pipes that contained 28 holes (1 mm).

The flow rates of gas and liquid phases were measured by flow meters and regulated by means of globe valves on the feed and bypass lines. A cartridge heater (2.54 cm OD $\times$ 1.5 m length) was installed vertically at the center of the bed in the test section. As a heating source, a cone shape vertical heater was used. The heater was constructed from a copper rod (1.50 m height $\times$ 0.03 m ID) axially drilled to accommodate a cartridge heater (1.33 m length $\times$ 0.012 m ID). Eight 1-mm diameter iron–constantan thermocouples were mounted in 2.0-mm wells and soldered in place, flush with the heater surface. The eight thermocouples were positioned 90° apart at the distance of 15-cm intervals from the top of the heater. The temperature of the heater surface was almost uniform and the effect of heater dimension could be neglected.[19] The temperature at the fluidized-bed proper was measured by the eight iron–constantan thermocouples (J-type), which were mounted at the center between the heater and the column at 0.15-m height intervals from the liquid distributor.

The heat transfer coefficient was determined by Eq. 1 from the knowledge of amount of heat supply and the mean temperature difference between the heater surface and the fluidized-bed proper.[11]

$$h = \frac{Q}{A(\overline{T_h - T_B})} \quad (1)$$

Twelve pressure taps were mounted flush with the wall of the column at 0.125-m height intervals from the liquid distributor. The extended bed height was taken as the point at which a change in the slope of the pressure drop plot was observed.[1,20] Bed porosity was determined from the knowledge of pressure drop, bed height, and properties of liquid and solid.[21,22] Throughout this study, aqueous solutions of carboxy methyl cellulose (CMC), whose apparent viscosity was varied from 1.0 to 38.0 $\times$ 10^{-3} Pa s, was used as the continuous liquid phase; compressed filtered air as the gas phase; and either polyethylene (PE) or polypropylene (PP) bead or plate, each with a density of 966.6, 877.3, 896.4, or 846.2 kg/m^3, respectively, as the solid phase. The contact angle of each particle with water was measured by means of an Erma contact angle meter (model G-1, Japan). The contact angle of PP was 84° and that of PE was 85°, respectively.[15,23] The apparent viscosity of liquid phase was determined with a Brookfield Synchrolectric Rotational Viscometer.[22,24] The properties of solid materials and liquid phase with fluid flow rate range are summarized in Tables 1 and 2, respectively.

Results and Discussions

Solid materials can be floated and fluidized by only gas flow in three-phase inverse fluidized beds of batch system ($U_L = 0$). In the batch system, effects of liquid viscosity on the heat transfer coefficient (h) can be seen in Figure 2, with the variation of gas velocity. In this figure, the value of h decreases gradually with increasing liquid viscosity (μ_L), but increases with increasing gas velocity (U_G) in all the cases studied. It is understood that the thickness of thermal boundary layer around the heater surface could increase with increasing liquid viscosity.[18,21,22] In addition, the contact time between the microeddy and the heater surface could increase with increasing liquid viscosity[25]; this, in turn, could lead to the decrease in the contacting frequency between them. Thus, the heat transfer coefficient decreases with increasing liquid viscosity. Deckwer[25] pointed out that the motion of microeddy is directly related to the heat transfer from the heater surface to the bed. The increase of gas velocity results in the increase in the amount of gas bubbles flowing upward as a discrete phase; thus, the turbulence between the immersed heater surface and the bed could increase. This consequently results in the increase of heat transfer coefficient in the beds.[26,27]

Effects of gas velocity (U_G) on the heat transfer coefficient in the continuous three-phase inverse fluidized beds can be seen in Figure 3. Note that the h value increases almost linearly with increasing U_G in all the cases studied. The rea-

Table 1. The Properties of Solid Materials Used in This Study

Particle	Shape	Average Diameter	Density (kg/m^3)
Polypropylene	Spheres	4 mm ID	877.3
Polypropylene	Plate	4 $\times$ 4 $\times$ 1 mm	846.2
Polyethylene	Spheres	4 mm ID	966.6
Polyethylene	Plate	4 $\times$ 4 $\times$ 2 mm	896.4

Table 2. Liquid Physical Properties and Fluids Flow Rate Range

	$\mu_{L,app} \times 10^3$ (Pa s)	$\sigma_L \times 10^3$ (N/m)	ρ_L (kg/m^3)	$U_G \times 10^2$ (m/s)	$U_L \times 10^2$ (m/s)
Pure water	0.96	72.9	1000	0.2–0.8	1–6
Aqueous solution of CMC 0.1 wt %	11	73.2	1001	0.2–0.8	1–6
Aqueous solution of CMC 0.2 wt %	24	73.3	1002	0.2–0.8	1–6
Aqueous solution of CMC 0.3 wt %	38	73.6	1003	0.2–0.8	1–6

son why h increases with increasing U_G can be that the bubbling phenomena become more vigorous with increasing U_G. It has been understood that the turbulence in the bed increases with increasing U_G, by increasing the breaking, coalescence, and splitting of bubbles due to the increase of gas holdup in three-phase inverse fluidized beds.[11]

Effects of liquid velocity (U_L) on the heat transfer coefficient can be seen in Figure 4. In this figure, h exhibits a maximum with increasing liquid velocity. This trend is very similar to that in the conventional three-phase fluidized beds.[1,20] The reason can be explained by means of solid holdup and solid flow regime. In other words, in the lower range of liquid velocity, the bed expands slowly and the turbulence resulting from the contacting among gas bubbles, solid materials, and liquid could increase, with increasing U_L; therefore h increases with increasing U_L. However, the solid holdup decreases significantly with a further increase in U_L, in the higher range of U_L. These result in insufficient contacting between the fluidized materials or fluid elements and the heater surface in the bed, and thus the liquid thin film around the heater surface cannot be eroded effectively. Therefore, h decreases with a further increase in U_L. In general, the gas is a dispersed phase and the liquid is a continuous phase to fluidize solid particles in three-phase inverse fluidized beds. Therefore, liquid flow may govern the flow structures in the bed. In addition, the fluidized materials may have a turbulence generating potential by hindering the continuous flow of the fluid element of liquid phase and rising bubbles.[17]

Effects of liquid viscosity (μ_L) on the heat transfer coefficient can be seen in Figure 5. In this figure, the heat transfer coefficient decreases gradually with increasing liquid viscosity. In three-phase inverse fluidized beds, the increase of liquid viscosity may lead to the decrease of bubble movement. This directly results in decrease of bubble holdup and turbulence causing from the bubbles. Moreover, the retardation of solid movement becomes considerable with increasing μ_L, which does not let the solid materials attack the thermal boundary layer around the heater surface and does not break the bubbles effectively in the bed.[20] Therefore, h decreases with increasing μ_L.

Effects of density of solid materials (ρ_p) on the heat transfer coefficient can be seen in Figure 6. In this figure, h increases with increasing density of solid materials. The increase of solid density could lead to the increase of turbulent intensity in the bed. The increase of turbulence intensity may come from the interruption the down flow of continuous liquid phase as well as the upward flow of dispersed gas phase by means of fluidized solid materials. Therefore, the contacting frequency between the fluid element and the heater surface increases and thus the contact time of them decreases, with increasing solid density. Based on the iso-

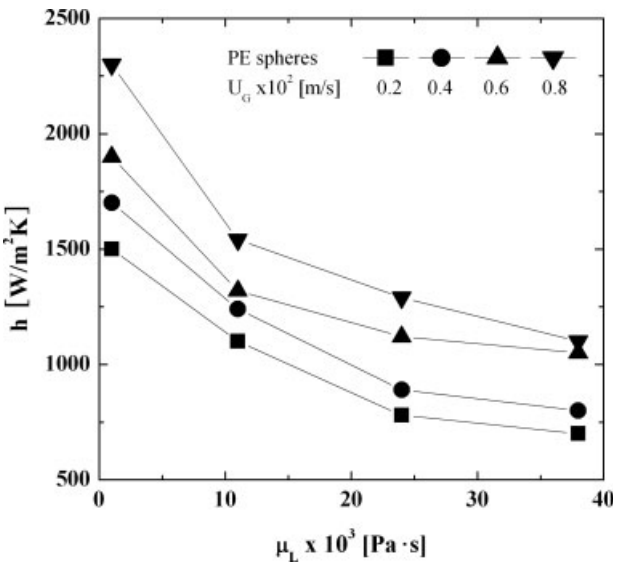

Figure 2. Effects of gas velocity and liquid viscosity on h in viscous three-phase inverse fluidized beds ($U_L = 0$).

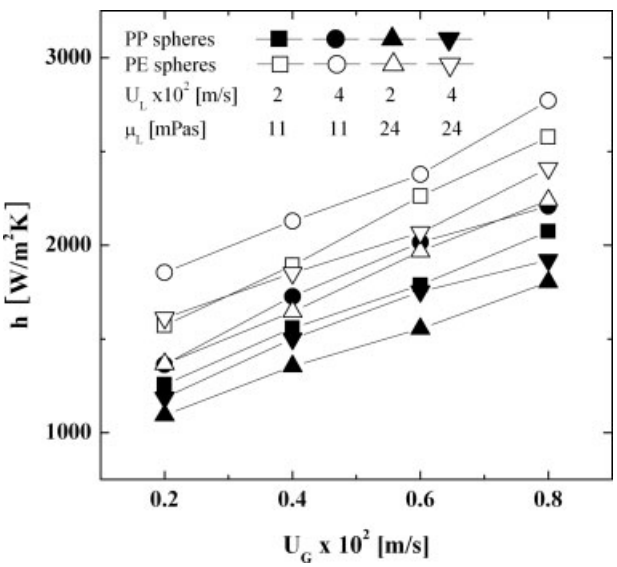

Figure 3. Effects of gas velocity on h in viscous three-phase inverse fluidized beds.

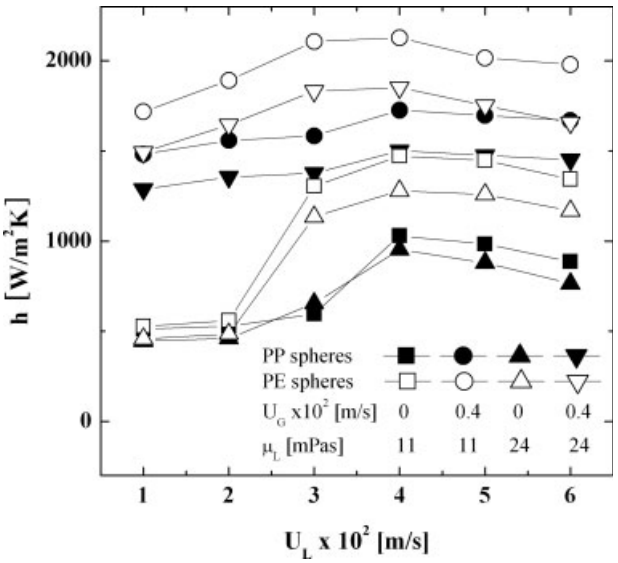

Figure 4. Effects of U_L on h in viscous three-phase inverse fluidized beds.

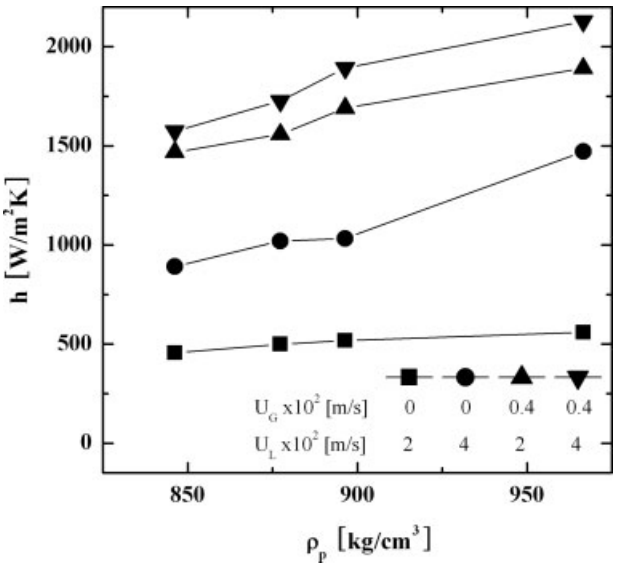

Figure 6. Effects of solid density on h in viscous three-phase inverse fluidized beds (μ_L = 24 mPas).

tropic turbulence theory, the heat flux from the heater surface to the fluid element is inversely proportional to the mean contact time of fluid element at the heater surface.[25]

Effects of bed porosity ($\varepsilon_G + \varepsilon_L$) on the heat transfer coefficient in three-phase inverse fluidized beds can be seen in Figure 7. In this figure, h exhibits a maximum with the increase in the bed porosity in the beds. The bed porosity at which h can attain its maximum increases with increasing U_G in the bed. It is noted that the bed porosity corresponding to the maximum h value is higher in the beds with the relatively denser solids (polyethylene) than that in the beds with the relatively lighter solid materials (polypropylene).

Since heat transfer would occur by means of the contacting of fluid element at the heater surface, the heat transfer can be controlled by the rate of renewal of fluid element of continuous phase, which may depend on the intensity of turbulence. Therefore, the average heat flux during the contact time θ of the liquid eddy at the heater surface can be written as[25]

$$q = \sqrt{\frac{\alpha_L}{\pi\theta}}\rho_L C_{PL}(T_w - T_i) \tag{2}$$

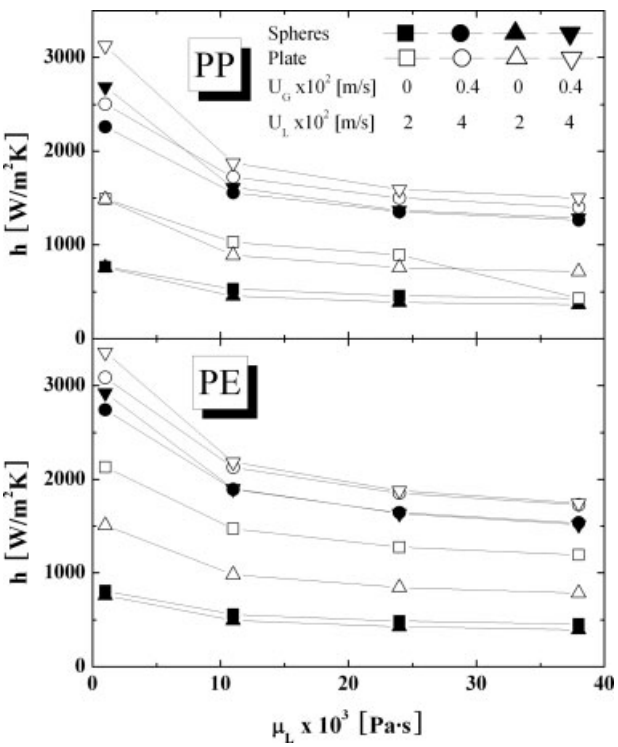

Figure 5. Effects of μ_L on h in viscous three-phase inverse fluidized beds.

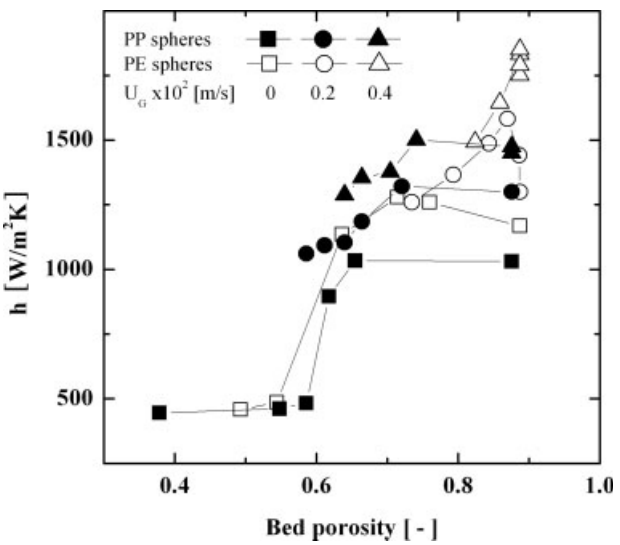

Figure 7. Effects of bed porosity on h in viscous three-phase inverse fluidized beds (μ_L = 24 mPas, U_G = 0.002 m/s).

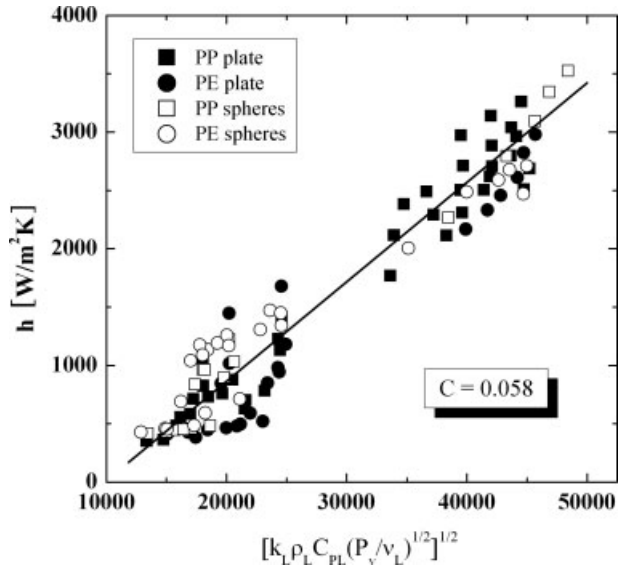

Figure 8. Determination of the proportional constant *C* from Eq. 9 in viscous three-phase inverse fluidized beds.

From the comparison of Eq. 2 with the common definition of heat transfer coefficient yields the following relation:

$$h \propto (k_L \rho_L C_{PL}/\theta)^{1/2} \tag{3}$$

Here, the contact time θ can be related to the length η and velocity scale ω of the microscale eddies based on the Kolmogoroff's isotropic turbulence theory,[28] with an assumption that relative turbulence intensity is roughly constant over the cross-section of the inverse fluidized bed within this experimental conditions.[29] Then, the contact time can be expressed as:

$$\theta = \eta/\omega \tag{4}$$

The length and velocity scale of microeddies can be correlated with the kinematic viscosity and the energy dissipation rate by means of dimensional analysis as Eqs. 5 and 6, respectively

$$\eta = (\nu_L^3/P_v)^{1/4} \tag{5}$$

$$\omega = (\nu_L P_v)^{1/4} \tag{6}$$

From Eqs. 3–6, the heat transfer coefficient can be expressed as

$$h \propto \left[k_L \rho_L C_{PL} (P_v/\nu_L)^{1/2}\right]^{1/2} \tag{7}$$

Since the energy dissipation rate per unit mass of continuous phase in the three-phase inverse fluidized beds can be written as Eq. 8,

$$P_v = [(U_L + U_G)(\rho_L \varepsilon_L + \rho_G \varepsilon_G + \rho_S \varepsilon_S) - (U_G \rho_G)]g/(\varepsilon_L \rho_L) \tag{8}$$

the heat transfer coefficient in three-phase inverse fluidized beds can be represented by substitution of Eq. 8 into Eq. 7 as

$$h = C[k_L \rho_L C_{PL}\{[(U_L + U_G)(\rho_L \varepsilon_L + \rho_G \varepsilon_G + \rho_S \varepsilon_S) - (U_G \rho_G)]g/\varepsilon_L \mu_L\}^{1/2}]^{1/2} \tag{9}$$

where C is the proportionality constant, which can be determined from the heat transfer coefficient data obtained in the present study. From the multiregression, the value of C was 0.058, as can be seen in Figure 8, with a correlation coefficient of 0.94.

For the practical application, the heat transfer coefficients between the immersed heater and the bed have been also well correlated in terms of dimensionless groups (Eq. 10). The correlation coefficient of Eq. 10 is 0.92 (Figure 9).

$$Nu = \frac{h d_p (1 - \varepsilon_S)}{k_L \varepsilon_S} = 38.52 \left(\frac{C_{PL} \mu_L}{k_L}\right)^{0.870} \left(\frac{d_p \rho_L (U_G + U_L)}{\mu_L \varepsilon_S}\right)^{1.018} \tag{10}$$

Concluding Remarks

The heat transfer coefficient between the immersed heater and the bed in three-phase inverse fluidized beds increased with increasing gas velocity or density of solid materials, but it decreased with increasing viscosity of continuous liquid medium, whereas it showed its maximum value with the variation of liquid velocity or bed porosity. The bed porosity at which the value of heat transfer coefficient attained its maximum increased with increasing gas velocity. The bed porosity corresponding to the maximum h value was higher in the beds with the relatively denser solid materials than that with the relatively lighter solid materials. The heat transfer coefficient was well analyzed and correlated by means of

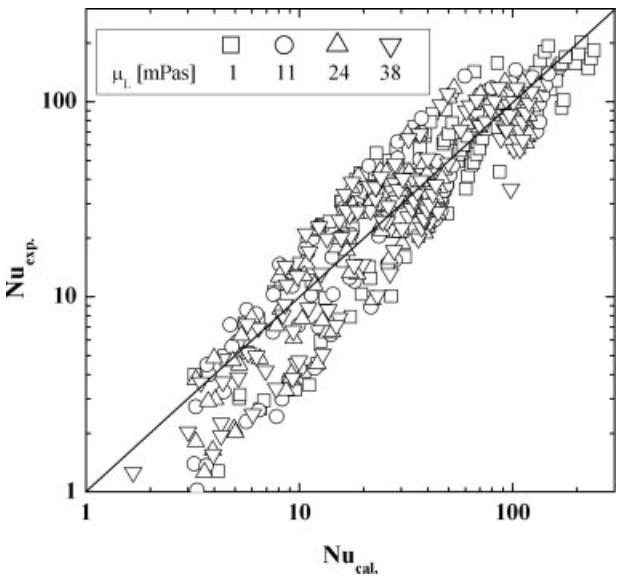

Figure 9. Correlation of heat transfer coefficient in viscous three-phase inverse fluidized beds.

energy dissipation rate in the bed based on the surface renewal concept at the heater surface. In addition, the heat transfer coefficient was well correlated in terms of dimensionless groups based on the isotropic turbulence theory.

Notation

A = surface area of heater, m^2
C_{PL} = heat capacity of liquid phase, kcal/(kg K)
d_P = particle diameter, m
g = acceleration due to gravity, m/s^2
h = heat transfer coefficient in three-phase inverse fluidized bed, $W/(m^2 K)$
k_L = conductivity of liquid phase, W/(m K)
P_v = specific energy dissipation rate, m^2/s^3
Q = heat flow, W
q = heat flux, W/m^2
T_B = boundary layer temperature, K
T_h = heater surface temperature, K
T_i = internal bed temperature, K
T_w = wall temperature, K
U_G = superficial gas velocity, m/s
U_L = superficial liquid velocity, m/s

Greek letters

α = thermal diffusivity, m^2/s
ε = phase holdup
η = length of microeddy, m
μ = viscosity, Pa s
ν = kinematic viscosity, m^2/s
π = the circular constant
θ = contact time, s
ρ = density, kg/m^3
ω = microeddy speed, m/s

Subscripts

G = gas phase
L = liquid phase
S = solid phase

Literature Cited

1. Fan LS. *Gas-Liquid-Solid Fluidization Engineering*. Boston: Butterworths,1989:368–374.
2. Legile P, Menard G, Laurent C, Thomas D, Bernis A. Contribution to the study of an inverse three-phase fluidized bed operating countercurrently. *Int Chem Eng*. 1992;32:41–50.
3. Garcia-Calderon D, Buffiere P, Moletta R, Elmaleh S. Anaerobic digestion of wine distillery wastewater in down-flow fluidized bed. *Water Res*. 1998;32:3593–3600.
4. Tokuyama H, Nii S, Kawaizumi F, Takahashi K. Removal of dilute nitric acid by anion exchange using a countercurrent multistage fluidized-bed column. *Ind Eng Chem Res*. 2002;41:3447–3453.
5. Kim SD, Kang Y. Hydrodynamics, heat and mass transfer in inverse and circulating three-phase fluidized-bed reactors for wastewater treatment. *Stud Surf Sci Catal*. 2006;159:103–108.
6. Song PS, Kang SH, Choi WK, Jung CH, Oh WZ, Kang Y. Recovery of copper powder from wastewater in three-phase inverse fluidized-bed reactors. *Stud Surf Sci Catal*. 2006;159:537–540.
7. Ibrahaim YAA, Breins CL, Margaritis A, Bergongnou MA. Hydrodynamic characteristics of a three-phase inverse fluidized-bed column. *AIChE J*. 1996;42:1889–1900.
8. Comte MP, Bastoul D, Hebrard G, Roustan M, Lazarova V. Hydrodynamics of a three-phase fluidized bed-the inverse turbulent bed. *Chem Eng Sci*. 1997;52:3971–3977.
9. Buffiere P, Moletta R. Some hydrodynamic characteristics of inverse three phase fluidized-bed reactors. *Chem Eng Sci*. 1999;54:1233–1242.
10. Lee DH, Epstein N, Grace JR. Hydrodynamic transition from fixed to fully fluidized beds for three-phase inverse fluidization. *Korean J Chem Eng*. 2000;17:684–690.
11. Cho YJ, Park HY, Kim SW, Kang Y, Kim SD. Heat transfer and hydrodynamics in two and three-phase inverse fluidized beds. *Ind Eng Chem Res*. 2002;41:2058–2068.
12. Tang WT, Fan LS. Gas-liquid mass transfer in a three-phase fluidized bed containing low density particles. *I&EC Res*. 1990;29:128–133.
13. Nikov I, Karamanev D. Liquid-solid mass transfer in inverse fluidized bed. *AIChE J*. 1991;37:781–784.
14. Nikolov V, Farag I, Nikov I. Gas-liquid mass transfer in bioreactor with three-phase inverse fluidized bed. *Bioprocess Biosyst Eng*. 2000;23:427–429.
15. Kim SW, Kim HT, Song PS, Kang Y, Kim SD. Liquid dispersion and gas-liquid mass transfer in three-phase inverse fluidized beds. *Can J Chem Eng*. 2003;81:621–625.
16. Renganathan T, Krishnaiah K. Liquid phase mixing in 2-phase liquid–solid inverse fluidized bed. *Chem Eng J*. 2004;98:213–218.
17. Cho YJ, Woo KJ, Kang Y, Kim SD. Dynamic characteristics of heat transfer coefficient in pressurized bubble columns with viscous liquid medium. *Chem Eng Proc*. 2002;41:699–706.
18. Shin KS, Song PS, Lee CG, Kang SH, Kang Y, Kim SD, Kim SJ. Heat-transfer coefficient in viscous liquid-solid circulating fluidized beds. *AIChE J*. 2005;51:671–677.
19. Lewis DA, Field RW, Xavier AM, Edwards D. Heat transfer in bubble columns. *Trans I Chem E*. 1982;60:40–48.
20. Kim SD, Kang Y. Heat and mass transfer in three-phase fluidized-bed reactors—an overview. *Chem Eng Sci*. 1997;52:3639–3660.
21. Kang Y, Suh IS, Kim SD. Heat transfer characteristics of three phase fluidized beds. *Chem Eng Commun*. 1985;34:1–13.
22. Kang Y, Fan LT, Kim SD. Immersed heater-to-bed heat transfer in liquid-solid fluidized beds. *AIChE J*. 1991;37:1101–1106.
23. Armstrong ER, Baker CGJ, Bergougnou MA. The effects of solid wettability on the characteristics of three-phase fluidization. In: Keairns DL, editor. *Fluidization Technology, Vol. 1*. Washington, DC: Hemisphere, 1976:405–412.
24. Schumpe A, Deckwer WD, Nigam KDP. Gas-liquid mass transfer in three-phase fluidized beds with viscous pseudoplastic liquids. *Can J Chem Eng*. 1989;67:873–878.
25. Deckwer WD. *Bubble Column Reactors*. New York: Wiley,1992: 260–268.
26. Chiu TM, Ziegler EN. Heat transfer in three phase fluidized beds. *AIChE J*. 1983;29:677–685.
27. Muroyama K, Fukuma M, Yasunishi A. Wall-to-bed heat transfer in liquid-solid and gas liquid solid fluidization beds. II. Gas-liquid-solid fluidized beds. *Can J Chem Eng*. 1986;64:409–418.
28. Hinze JD. *Turbulence*, 2nd ed. New York: McGraw-Hill, 1975.
29. Deckwer WD. On the mechanism of heat transfer in bubble column reactors. *Chem Eng Sci*. 1980;35:1341–1348.

Manuscript received Aug. 6, 2006, and revision received July 18, 2007.